Recycling Intergalactic and Interstellar Matter
IAU Symposium Series, Vol. 217, 2004
Pierre-Alain Duc, Jonathan Braine and Elias Brinks, eds.

Mass Spectrum of a Starburst

Jan Palouš, Richard Wünsch, Soňa Ehlerová

Astronomical Institute, Academy of Sciences of the Czech Republic

Abstract. The fragmentation of supershells and filaments driven by a superwind in a starburst region produces clumps with a mass spectrum approximated by a power law. Its spectral index is close to -2.3. We present results of computer simulations using the thin shell approximation, which are compared to 3D hydrodynamical simulations with self-gravity using the ZEUS computer code. In a low density medium the fragmentation time-scale is comparable to the collisional time-scale, and consequently collisions change the mass spectra of fragments to less steep values. In high density environments collisional time-scales are much longer and the mass spectrum results from gravitational fragmentation of expanding sheets and filaments.

1. Introduction

The stellar IMF has been approximated by a power-law with a slope $\alpha = -2.35$ (Salpeter, 1955). No convincing observational evidence of place to place variations has been found up to now, but uncertainities in the slope are large (Kroupa et al. 1993; Scalo, 1998). The universal IMF (Kroupa, 2001) has two changes in the power-law index near 0.08 $M_\odot$ and 0.5 $M_\odot$: $\alpha = (0.3 \pm 0.7;\ 1.3 \pm 0.5;\ 2.3 \pm 0.3;\ 2.3 \pm 0.7)$ for mass intervals $(0.01 - 0.08;\ 0.08 - 0.5;\ 0.5 - 1.0;\ > 1)\ M_\odot$. The mass spectrum of cold cores of molecular clouds with densities $\geq 10^5$ cm^{-3} (Tachihara et al., 2002) is approximated with the following power-law slopes: $\alpha = (1.25;\ 2.5;\ 3.6)$ for mass intervals $(< 10;\ 10 - 60;\ > 60)\ M_\odot$. The transformation of cold cores to protostars with a mass-independent efficiency probably produces a mass spectrum similar to the universal IMF. In this paper we derive the mass spectrum of fragments of supershells and filaments expanding in a starburst region. We show that it is similar to the universal IMF as given by Kroupa (2001): it has a proper slope at the high mass end, which changes to a less steep profile towards lower masses.

2. Gravity versus pressure and stretching

Inside a thin layer,gravity competes with the internal pressure and the stretching connected to its expansion (see Fig. 1). The stability of the layer is given in a linear approximation by the dispersion relation (Elmegreen, 1994; Wünsch &

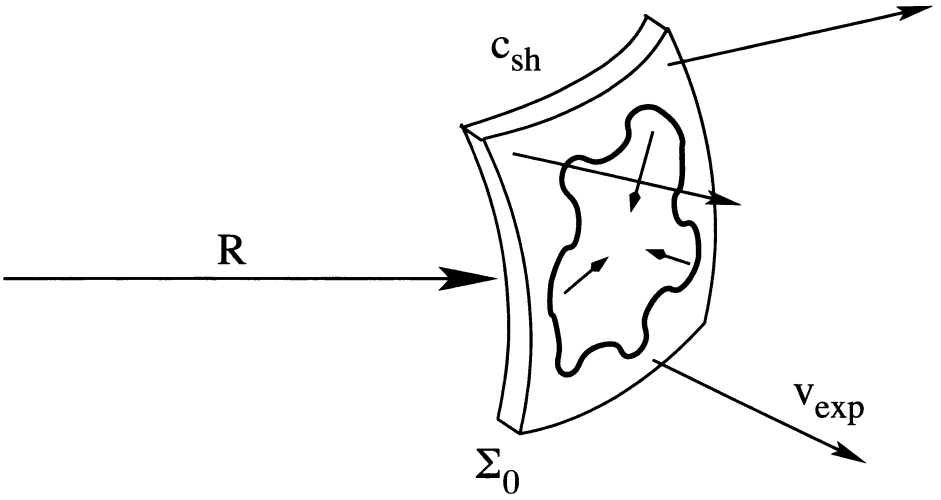

Figure 1. The expanding thin layer. R is the radius of the curvature, V_{exp} is the expansion velocity, Σ_0 is the unperturbed column density and c_{sh} is the speed of sound inside of the layer.

Palouš, 2001)

$$\omega = -\frac{3V_{exp}}{R} + \sqrt{\frac{V_{exp}^2}{R^2} - \frac{c_{\rm sh}^2\eta^2}{R^2} + \frac{2\pi G\Sigma_0\eta}{R}}, \quad (1)$$

where G is the constant of gravity, R is the curvature radius of the thin layer, V_{exp} is its expansion speed, Σ_0 is its column density, $c_{\rm sh}$ is the speed of sound within the layer and $\eta = 2\pi R/\lambda$ is the wavenumber. Perturbations grow if the right side of eq. (1) is real and positive. The last term with G in eq. (1) represents the influence of gravity, the term with $c_{\rm sh}^2$ gives the influence of the pressure and the remaining two terms come from a stretching due to an expansion. The pressure always dominates in the short-wavelength modes and makes them stable. Long-wavelength modes are stabilized by the stretching, when R is small and V_{exp} is large. When the layer decelerates because of mass accumulation, the gravity term dominates intermediate modes between short-wavelength modes stabilized by pressure and long-wavelength modes stabilized by stretching. These gravity-dominated modes form self-gravitating fragments (see the left panel of Fig. 2). The time evolution of the most unstable fragment is given in the right panel of Fig. 2. Assuming continuous energy input L, the self-similar solution for R, V and Σ_0 is given by Castor et al. (1975). With the self-similar solution inserted in the dispersion relation (1) we find the time t_b when the instability of the layer appears for the first time (see Fig. 2):

$$t_{\rm b} = 28.8 \times \left(\frac{c_{\rm sh}}{\rm km\ s^{-1}}\right)^{\frac{5}{8}} \times \left(\frac{L}{10^{51}\ \rm erg\ Myr^{-1}}\right)^{-\frac{1}{8}} \times \left(\frac{\mu}{1.3}\frac{n}{\rm cm^{-3}}\right)^{-\frac{1}{2}} \rm Myr, \quad (2)$$

where n is the density of the ambient medium and μ is its mean atomic weight in amu. Values of the time t_b for low and high densities are given in Table 1.

https://doi.org/10.1017/S0074180900197839 Published online by Cambridge University Press

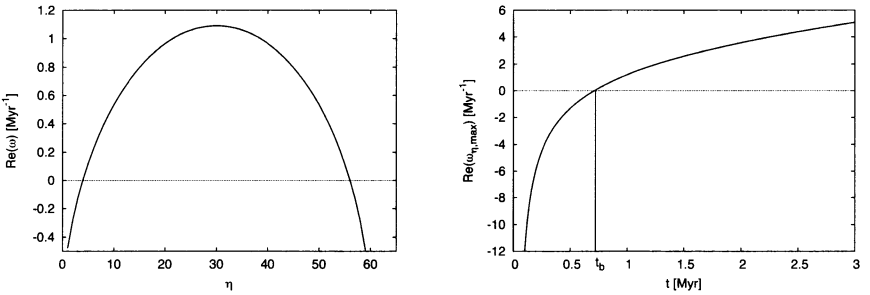

Figure 2. The dispersion relation (1) (left panel) and the time evolution of the most unstable mode (right panel).

In low densities, $n \leq 1$ cm^{-3}, the time-scale t_b is a few times 10^6 yr, therefore the gravitational fragmentation is a rather slow process, but in high densities, $n \geq 10^6$ cm^{-3}, it is very fast with the time-scale less that 10^4 yr.

n [cm^{-3}]	$c_{\rm sh}$ [km s^{-1}]	0.3	0.5	1.0
10^{-1}		43	59	91
1		14	19	29
10^6		0.01	0.02	0.03

Table 1. Values of $t_{\rm b}$ in Myr as defined by the formula (2) for $L = 10^{51}$ erg Myr^{-1} and $\mu = 1.3$ amu.

3. The mass spectrum of fragments

The mass spectrum of fragments can be derived using the method described by Palouš et al. (2003). The wavenumber of the fastest growing fragment is $\eta_{\rm max} = \frac{\pi G \Sigma_0 R}{c_{\rm sh}^2}$ and its mass at $t_{\rm b}$ is

$$m_{\rm max} \sim G^{-2} c_{\rm sh}^{29/8} L^{-1/8} n^{-1/2} \mu^{-1/2}. \quad (3)$$

Fig. (3) shows the dependence of the mass spectra on n, L and c_{sh}. We see the shift of $m_{\rm max}$ to lower masses for higher densities n, the sensitive dependence of fragment masses on $c_{\rm sh}$, and a small shift with luminosity L. The time evolution of the spectral index α is shown in Fig. (4). The time is in units $t_{\rm b}$ defined by eq. (2) and given in Table 1. Independently of $L, c_{\rm sh}$ and n the value of the spectral index reaches a value $\alpha = 2.25 - 2.4$ for $t \geq 4\ t_{\rm b}$. For earlier times the mass spectrum is flatter, but the power law approximation is poor.

4. The thin layer approximation

Numerical simulations using the thin layer approximation has been performed using the code described by Ehlerová & Palouš (2002) and Elmegreen et al.

https://doi.org/10.1017/S0074180900197839 Published online by Cambridge University Press

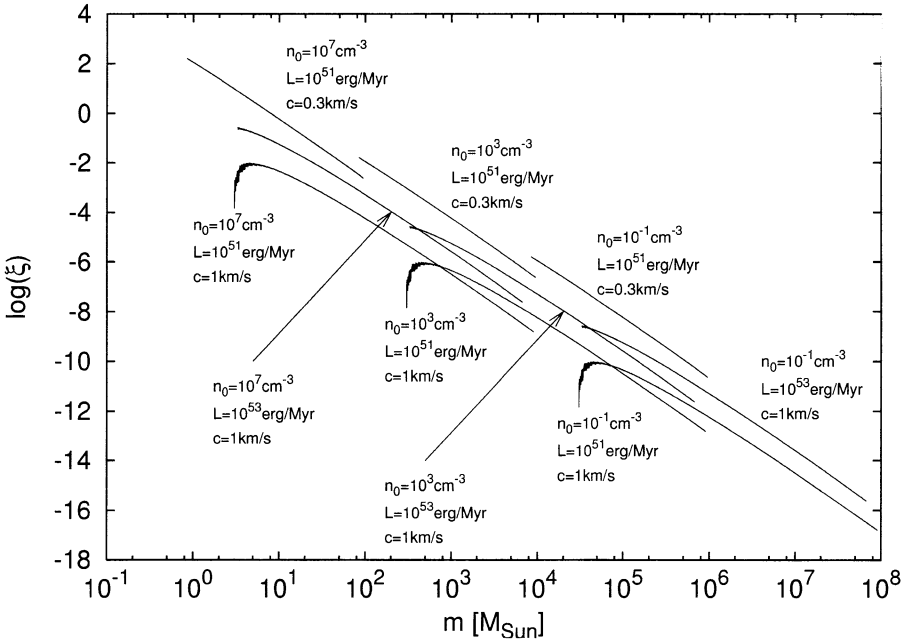

Figure 3. The mass spectrum of fragments of an expanding thin layer at time $5t_b$.

(2002). They include effects, which are neglected in the analytical solution, suvh as the pressure of the ambient medium and the finite speed of sound in the ambient medium. Values $R(t), V_{exp}(t), \Sigma_{\rm sh}(t)$ from simulations are inserted in equation (2) and the mass spectrum of fragments is calculated. The power-law index α is fitted to the central part of the declining region of the spectrum. Results are shown in Fig. (4), together with the self-similar solution. There is an agreement between analytical and numerical solutions. Independently of inclusion of the external pressure, of the finite speed of sound in the ambient medium, and of the value of $L, c_{\rm sh}$ and n, the spectral index has a value $\alpha = 2.25 - 2.4$ for $t \geq 4t_{\rm b}$. For earlier times the mass spectrum is flatter.

5. 3-dimensional simulations of hydrodynamical and Poisson equations using ZEUS and Šemík codes

Here we show first results of the 3-dimensional simulations of hydrodynamical equations using the ZEUS code (Stone & Norman, 1992) with the gravitational potential computed by the code Šemík developed by Wünsch (2003). In agreement with the analytical solution, at some point of the evolution the accumulated gas in the shock wave starts to form fragments. Some fragments are gravitationally bound, some are not and later dissolve. In Fig. (5) we show the surface density distribution on the sheet surface and the resulting mass spectrum of gravitationally bound and unbound fragments. Its slope is near to $\alpha = -2.3$.

https://doi.org/10.1017/S0074180900197839 Published online by Cambridge University Press

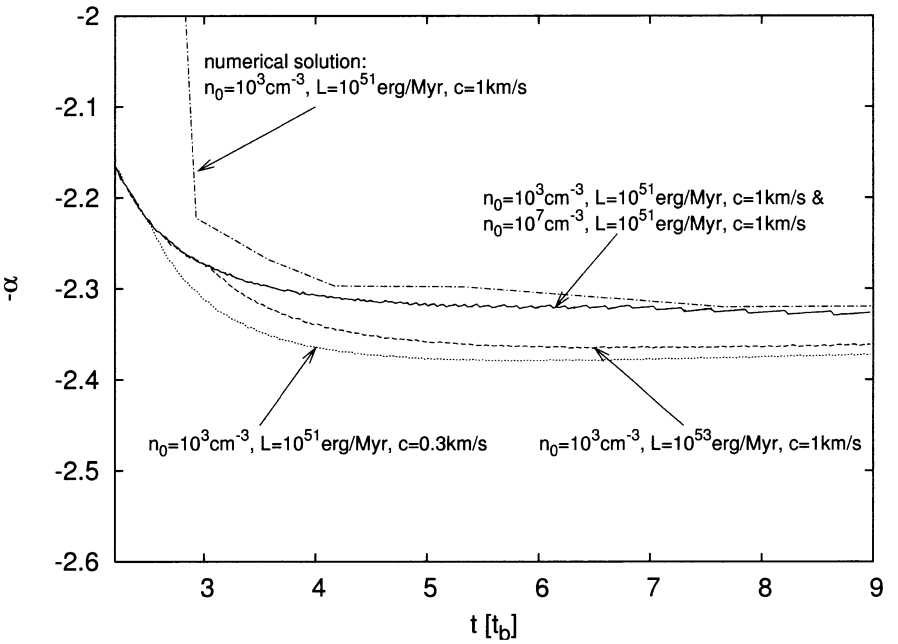

Figure 4. The time evolution of the spectral index α.

6. Discussion and conclusions

Our conclusions are based on numerical simulations using the thin layer approximation and 3-dimensional hydrodynamical simulations using ZEUS code complemented with the gravitational potential derived by the code Šemík. The gravitational fragmentation of expanding supershells is important for production of clumps if the time-scale $t_{\rm b}$, which is the dynamical time-scale for the collapse of fragments in supershells and sheets in the ISM, is shorter than the collisional time-scale $t_{\rm a}$. If the gravitational fragmentation is slow (i.e. $t_{\rm b}$ long), collisions play a more important role and shape the spectrum of clumps. In a low density medium, (0.1 - 1) cm^{-3}, the mass range of fragments $(10^4 - 10^7)$ M$_\odot$ corresponds to masses of molecular clouds, but $t_{\rm b}$ is 10-100 Myr and $t_{\rm a}/t_{\rm b} \sim 1$. Therefore, the influence of the gravitational collapse of supershells and sheets on the mass spectrum of fragments is restricted by the collisional agglomeration. Fragments form with the calculated mass-spectrum, but the collisional agglomeration changes it later to less steep values, which correspond to observed slopes $\alpha = 1.5 - 2.0$, since any process of merging decreases the number of low-mass clumps and increases the number of high-mass clumps. In high density environments of molecular cloud cores, $(10^6 - 10^7)$ cm^{-3}, gravitational time-scales are short, $(10^3 - 10^4)$ yr. Fragments in these environments have masses in the range between (1 - 100) M$_\odot$. Collisional time-scales (Elmegreen & Shadmehri, 2003) are longer than typical $t_{\rm b}$. This implies, that gravitational fragmentation is important and shapes the mass spectrum of protostars. As shown above, the

https://doi.org/10.1017/S0074180900197839 Published online by Cambridge University Press

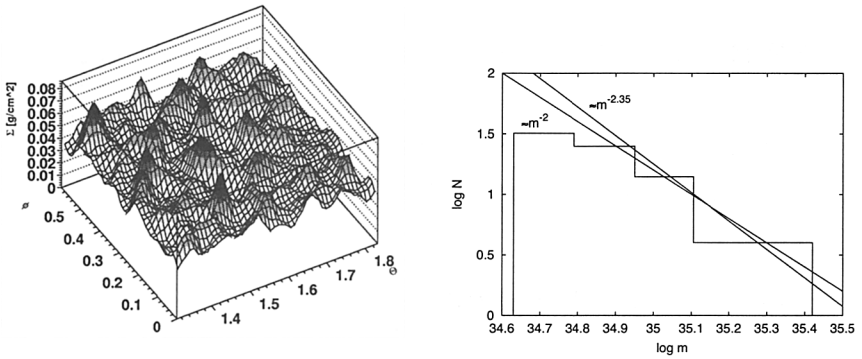

Figure 5. The surface density distribution on an expanding sheet(left panel), and the mass spectrum of fragments (right panel).

gravitational fragmentation of expanding supershells and sheets gives a power-law with a slope of $\alpha = 2.25 - 2.4$.

Acknowledgments. The authors gratefully acknowledge financial support by the Grant Agency of the Academy of Sciences of the Czech Republic under grant No. B3003106, and support via projects of the Academy of Sciences of the Czech Republic Nos. K1048102 and AV0Z 1003909.

References

Castor, J., McCray, R., Weaver, R., 1975, ApJ, 200, L107

Ehlerová, S., Palouš, J., 2002, MNRAS, 330, 1022

Elmegreen, B. G., 1994, ApJ, 427, 384

Elmegreen, B. G., Shadmehri, M, 2003, MNRAS, 338, 817

Kroupa, P., 2001, MNRAS, 322, 231

Kroupa, P., Tout, C. A., Gilmore, G., 1993, MNRAS, 262, 545

Palouš, J., Wünsch, R. & Ehlerová, S., 2003, Ap&SS, 284, 873

Salpeter, E. E., 1955, ApJ, 121, 161

Scalo, J. M., 1998, in The Stelar Initial Mass Function, eds G. Gilmore and D. Howell, ASP Conf. Ser., Vol 142, Astron. Soc., San Francisco, p. 201

Stone, J. M., Norman, M. L., 1992, ApJS, 80, 753

Tachihara, K., Onishi, T., Mizuno, A., Fukui, Y., 2002, A&A, 385, 909

Wünsch, R., 2003, PhD thesis, Charles University, Prague

Wünsch, R., Palouš J., 2001, A&A, 374, 746